

Quadruple, 4-segment, triple sector “Y-shaped stents” in complex hilar cholangiocarcinoma after cholangitis from plastic stents



Mohamed A. Abdallah, MD, Martin L. Freeman, MD, Stuart K. Amateau, MD, PhD, Matthew R. Krafft, MD

A 70-year-old Asian-American woman with a history of unresectable, locally advanced Bismuth-Corlette classification type IV perihilar cholangiocarcinoma initially presented with ascending cholangitis.

Four weeks before presentation to our institution, the patient underwent percutaneous transhepatic biliary drainage at an outside hospital for biliary drainage after index ERCP failed to access the left and right intrahepatic bile ducts. One week after that, the patient presented to our institution with ascending cholangitis. ERCP was performed, revealing diffuse cholangitis. Salvage therapy included placement of 4 transpapillary biliary plastic stents into the right posterior sectoral duct (RP), right anterior sectoral duct (RA), left lateral segment II (LL-II), and left lateral segment III (LL-III).

Evaluation by medical and surgical oncology recommended against surgical resection and palliative chemotherapy owing to the patient's poor performance status. Therefore, the patient was referred for palliative endoscopic biliary drainage with an uncovered, laser-cut, nonforeshortening 6F delivery system, metallic stents. MRCP was not performed before the planned ERCP because the decision was made to drain all accessible liver sectors owing to the presence of cholangitis.

A duodenoscope (TJF-Q180B; Olympus America, Center Valley, Pa, USA) was advanced to the second portion of the duodenum. The 4 previously placed transpapillary biliary

plastic stents were removed using a snare (Fig. 1). The common bile duct was cannulated using a bending cannula (SwingTip; Olympus America). Cholangiogram



Figure 2. Fluoroscopic image showing Bismuth-Corlette type IV perihilar cholangiocarcinoma and diffuse intrahepatic biliary ductal dilation.

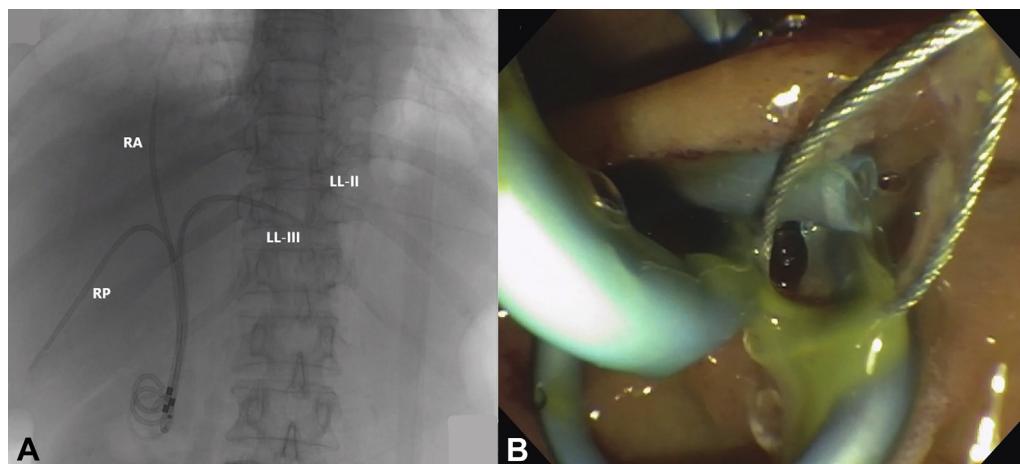


Figure 1. **A,** Fluoroscopic image showing 4 transpapillary biliary stents in the right posterior sectoral duct, right anterior sectoral duct, left lateral segment II, and left lateral segment III. **B,** Endoscopic image showing removal of the plastic stents before self-expanding metal stent insertion. *RP*, Right posterior; *RA*, right anterior; *LL-II*, left lateral segment II; *LL-III*, left lateral segment III.

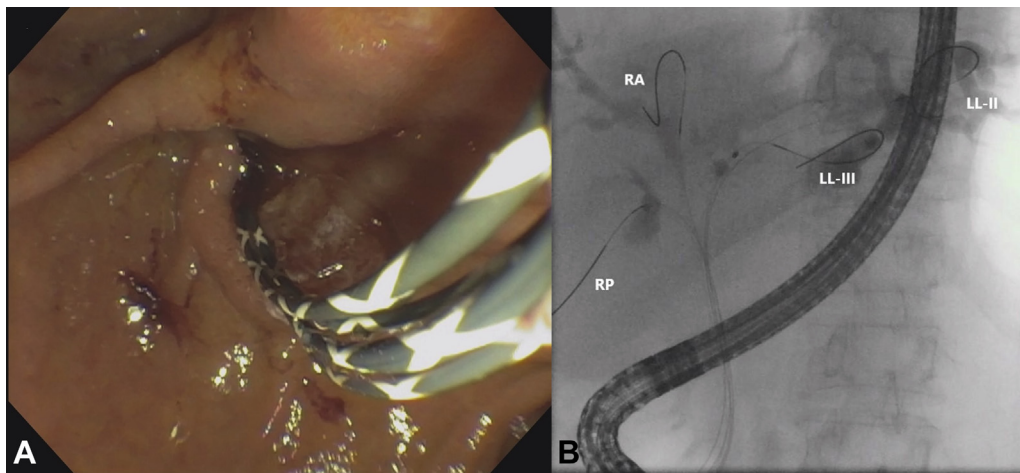


Figure 3. **A**, Endoscopic and **(B)** fluoroscopic image showing four 0.025-inch \times 450-cm straight Visiglide guidewires in each of the 4 segmental intrahepatic ducts. *RP*, Right posterior; *RA*, right anterior; *LL-II*, left lateral segment II; *LL-III*, left lateral segment III.

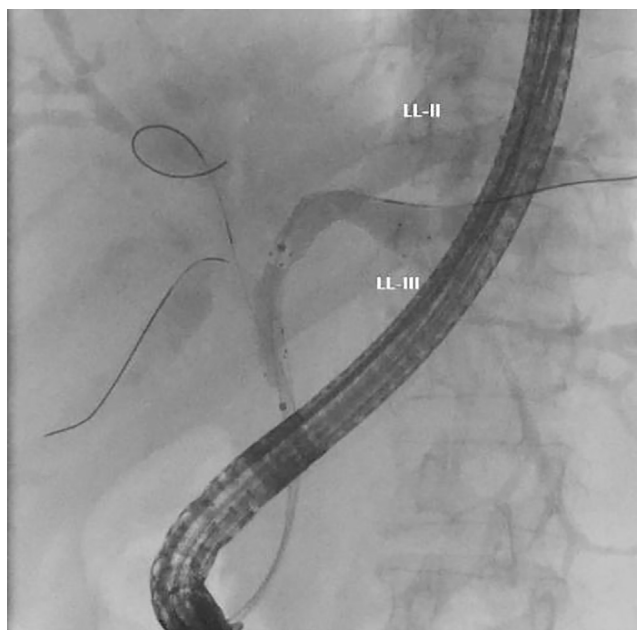


Figure 4. Fluoroscopic image showing an intraductal 10-mm \times 6-cm uncovered self-expanding metal stent that was advanced over the wire, passing through a slit in the left lateral segment III self-expanding metal stent and into the left lateral segment II, forming a Y-shaped intraductal stent-in-stent. *LL-II*, Left lateral segment II; *LL-III*, left lateral segment III.

showed typical biliary confluence anatomy with a Bismuth type IV perihilar tumor and diffuse intrahepatic biliary ductal dilation (Fig. 2). A total of four 0.025-inch \times 450-cm straight guidewires (Visiglide; Olympus America) were passed into each of the 4 segmental intrahepatic ducts from which the 4 plastic stents were just removed (ie, *RP*, *RA*, *LL-II*, and *LL-III*) (Fig. 3). The confluence (takeoff) of each sectoral branch duct was dilated to 6 mm using a biliary balloon dilatation catheter (Hurricane RX; Boston Scientific; Marlborough, Mass, USA). Each of the 4 sectoral ducts was swept with a 9-



Figure 5. Fluoroscopic image showing an intraductal 10-mm \times 8-cm uncovered self-expanding metal stent that was deployed through a slit in the left lateral segment III self-expanding metal stent, terminating in the right posterior sectoral duct, forming a second Y-shaped intraductal stent-in-stent. *RP*, Right posterior; *LL-II*, left lateral segment II; *LL-III*, left lateral segment III.

mm retrieval balloon catheter (Extractor pro RX-S, Boston Scientific) to clear residual sludge and pus from each duct.

Under fluoroscopic guidance, an intraductal 10-mm \times 8-cm uncovered self-expanding metal stent (SEMS) (Zilver 635, Cook Medical, Bloomington, Ind, USA) was deployed across the hilum, spanning from the common hepatic duct into *LL-III*. The *LL-III* uncovered SEMS was cannulated over the wire using the SwingTip cannula. The guidewire was poked through a slit in the *LL-III* SEMS, passing into *LL-II*. A 10-mm \times 6-cm uncovered Zilver 635 SEMS was advanced over the wire, passing through the slit in *LL-III* SEMS and into *LL-II*, forming a Y-shaped intraductal

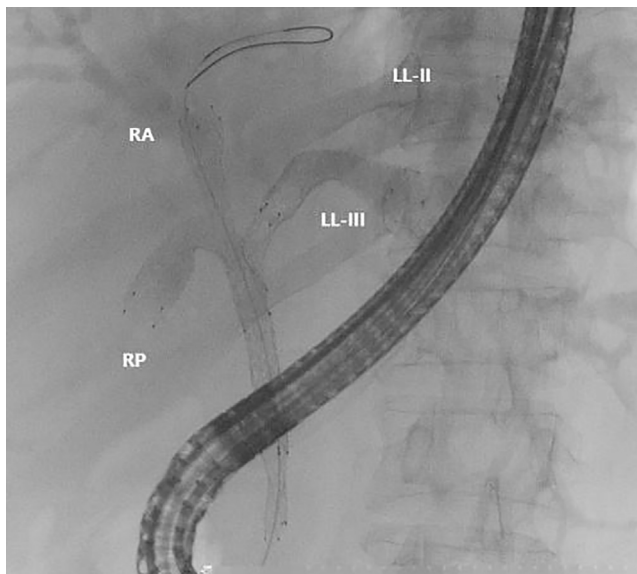


Figure 6. Fluoroscopic image showing an intraductal 10-mm × 8-cm uncovered self-expanding metal stent that was deployed through a slit in the left lateral segment III self-expanding metal stent, terminating in the right anterior sectoral duct, forming a third Y-shaped intraductal stent-in-stent. *RP*, Right posterior; *RA*, right anterior; *LL-II*, left lateral segment II; *LL-III*, left lateral segment III.

stent-in-stent (Fig. 4). The distal tip of the second SEMS (*LL-II*) was intentionally deployed proximal to the biliary bifurcation, so as not to impede creation of more Y-shaped intraductal stent-in-stent configurations in the right lobe of the liver.

After creation of the first Y-shaped stent-in-stent in *LL-II/III*, we turned our attention to the obstructed *RA* and *RP*. The *LL-III* SEMS was recannulated using the SwingTip cannula; a guidewire was advanced through a slit in the SEMS, passing into the *RP*. A 10-mm × 8-cm uncovered Zilver 635 SEMS was deployed through the slit in the *LL-III* SEMS, terminating in the *RP*, forming a second Y-shaped intraductal stent-in-stent (Fig. 5). The process was again repeated such that the *RA* was drained via passage of a 10-mm × 8-cm uncovered Zilver 635 SEMS through the *LL-III* SEMS, forming a third Y-shaped intraductal stent-in-stent (Fig. 6).

The final stent configuration consisted of the initial SEMS extending from the common hepatic duct to *LL-III*, with 3 penetrating/traversing SEMSs terminating in *LL-II*, *RP*, and *RA* (Fig. 7). Four-week follow-up revealed normalization of total bilirubin, alanine transaminase, and aspartate transaminase and a significant decrease in alkaline phosphatase levels without cholangitis, with CT showing stable SEMS position (Fig. 8). The patient elected not to pursue further therapy and transitioned to home hospice care.

Most patients with perihilar cholangiocarcinoma present with unresectable disease, and endoscopic drainage provides an optimal therapeutic modality for biliary obstruction and cholangitis.^{1,2} In this setting, SEMSs are associated with higher technical success, fewer adverse events, and better survival compared with plastic stents.^{3,4}

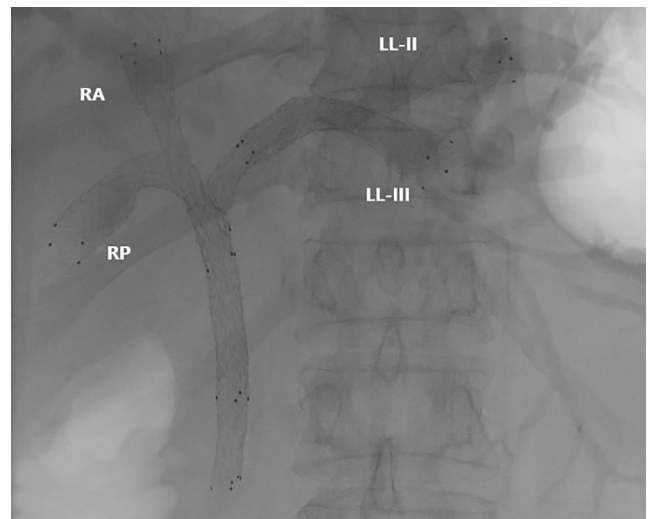


Figure 7. Fluoroscopic image showing the initial uncovered self-expanding metal stent extending from the common hepatic duct to the left lateral segment III, with 3 penetrating/traversing self-expanding metal stents terminating in the left lateral segment II, right posterior sectoral duct, and right anterior sectoral duct. *RP*, Right posterior; *RA*, right anterior; *LL-II*, left lateral segment II; *LL-III*, left lateral segment III.

In this case, we expanded upon the Y-shaped intraductal stent-in-stent technique, successfully completing a triple Y-shaped configuration. All biliary sectoral branches that previously housed plastic stents were exchanged for SEMSs to prevent future episodes of cholangitis from occurring in the previously instrumented sectors. All 4 ducts were cannulated with a guidewire, facilitated by using a steerable catheter (Swingtip) before the deployment of any SEMS to guide insertion of subsequent SEMSs. All SEMSs were inserted suprapapillary because suprapapillary placement is associated with longer stent patency, lower risk of cholangitis (from presumed enteric-biliary reflux), and decreased risk of pancreatitis (from pancreatic duct orifice compression), compared with transpapillary SEMS insertion.⁵

The performance of the stent-in-stent versus side-by-side technique for biliary drainage in a meta-analysis of 4 studies ($N = 158$) was similar with respect to rates of successful placement, successful drainage, early adverse events, late adverse events, and stent occlusions.⁶ We elected to use the stent-in-stent technique to avoid potential stent overcrowding and compression of stents by one another. In addition, in our patient, the stent-in-stent technique was selected over side-by-side stents to facilitate endoscopic reintervention, including intraductal radiofrequency ablation of tumor ingrowth.⁷⁻⁹

Use of SEMSs for biliary stent placement is complex and needs to be performed by providers with expertise and experience in the management of malignant hilar biliary obstruction. Adverse events of SEMS insertion can be seen in up to 30% of patients and can include inappropriate placement in a resectable lesion, cholangitis secondary to placement in the wrong segmental ducts, tumor

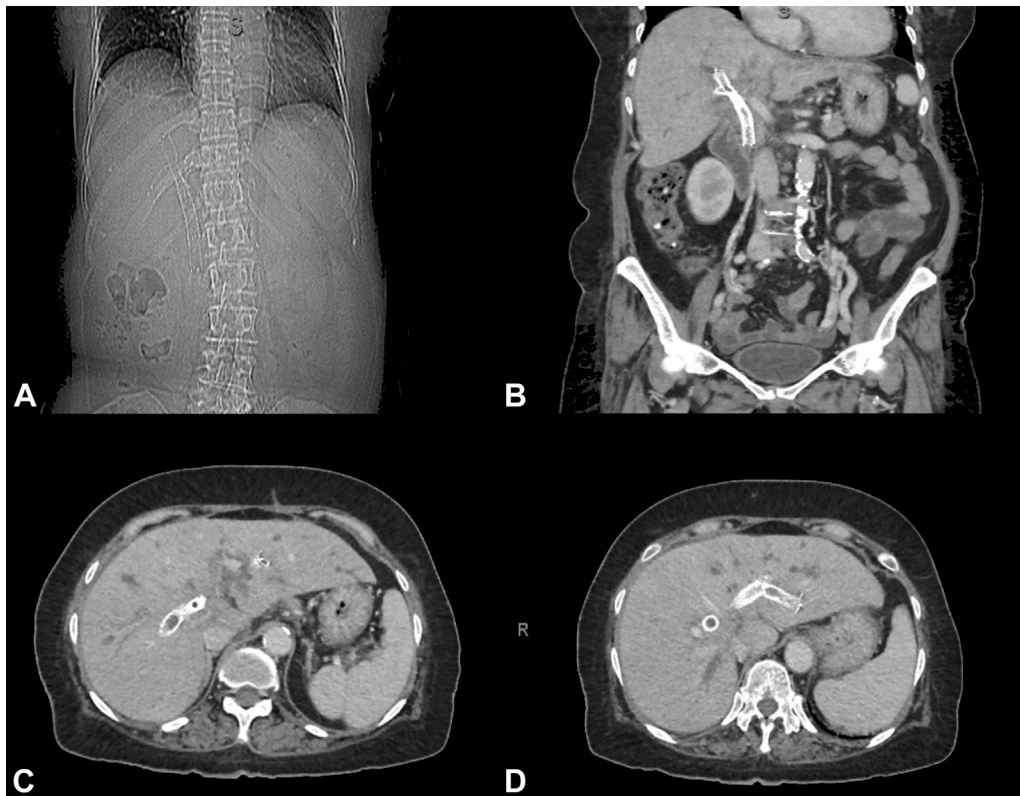


Figure 8. CT obtained 4 weeks after insertion of uncovered self-expanding metal stents (SEMSs). **A**, Scout image showing the 4 previously placed SEMSs: 1 extending from the common hepatic duct to the left lateral segment III (LL-III), with 3 penetrating/traversing SEMSs terminating in left lateral segment II (LL-II), right posterior sectoral duct (RP), and right anterior sectoral duct (RA). **B**, Coronal view showing SEMS to LL-III with SEMS take-off to RP. **C**, Cross-sectional view showing SEMS to RA and RP. **D**, Cross-sectional view showing SEMS to LL-II, L-III, and RA.

ingrowth, reactive hyperplasia, stone formation, and bleeding from SEMS erosion into vessels (Video 1, available online at www.giejournal.org).⁹

DISCLOSURE

Dr Amateau serves as a consultant for Boston scientific, Merit Endoscopy, US Endoscopy/Steris, a consultant and advisor for Olympus, and a consultant and research support for Cook Medical. All other authors disclosed no financial relationships.

Abbreviations: LL-II, left lateral segment II; LL-III, left lateral segment III; RA, right anterior sectoral duct; RP, right posterior sectoral duct; SEMS, self-expanding metal stent.

REFERENCES

1. Kerssirichairat T, Arain MA, Attam R, et al. Endoscopic drainage of >50% of liver in malignant hilar biliary obstruction using metallic or fenestrated plastic stents. *Clin Transl Gastroenterol* 2017;8:e115.
2. Razumilava N, Gores GJ. Cholangiocarcinoma. *Lancet* 2014;383:2168-79.
3. Perdue DG, Freeman ML, DiSario JA, et al. Plastic versus self-expanding metallic stents for malignant hilar biliary obstruction: a prospective

multicenter observational cohort study. *J Clin Gastroenterol* 2008;42:1040-6.

4. Sangchan A, Kongkasame W, Pugkhem A, et al. Efficacy of metal and plastic stents in unresectable complex hilar cholangiocarcinoma: a randomized controlled trial. *Gastrointest Endosc* 2012;76:93-9.
5. Huang X, Shen L, Jin Y, et al. Comparison of uncovered stent placement across versus above the main duodenal papilla for malignant biliary obstruction. *J Vasc Interv Radiol* 2015;26:432-7.
6. Hong W, Chen S, Zhu Q, et al. Bilateral stenting methods for hilar biliary obstructions. *Clinics (Sao Paulo)* 2014;69:647-52.
7. Wadsworth CA, Westaby D, Khan SA. Endoscopic radiofrequency ablation for cholangiocarcinoma. *Curr Opin Gastroenterol* 2013;29:305-11.
8. Freeman ML. Endoscopic management of hilar bile duct strictures Q&A. *ASGE Connection* 2014;2:1-7.
9. Tiewala MA, Freeman ML. Self-expanding metallic stents for malignant hilar biliary obstruction. In: *Self-Expandable Stents in the Gastrointestinal Tract*. New York: Springer; 2013. p. 217-33.

Division of Gastroenterology, Hepatology, and Nutrition, University of Minnesota, Minneapolis, Minnesota.

If you would like to chat with an author of this article, you may contact Dr Abdallah at abdal088@umn.edu.

Copyright © 2022 American Society for Gastrointestinal Endoscopy. Published by Elsevier Inc. This is an open access article under the CC BY-NC-ND license (<http://creativecommons.org/licenses/by-nc-nd/4.0/>).

<https://doi.org/10.1016/j.vgie.2021.09.009>